

Electronic Supplementary Material (ESI) for Journal of Materials Chemistry A  
This journal is © The Royal Society of Chemistry 2021

## Supporting Information

### Heterostructured graphene oxide membranes with tunable water-capture coatings for highly selective water permeation

Zhiming Zhang<sup>ab</sup>, Hong Wu<sup>\*abde</sup>, Ying Li<sup>ab</sup>, Yue Liu<sup>ab</sup>, Chenliang Cao<sup>ab</sup>, Hongjian Wang<sup>ab</sup>, Meidi Wang<sup>ab</sup>,  
Fusheng Pan<sup>\*abcd</sup> and Zhongyi Jiang<sup>\*abcd</sup>

<sup>a</sup> Key Laboratory for Green Chemical Technology of Ministry of Education, School of Chemical  
Engineering and Technology, Tianjin University, Tianjin 300072, China

<sup>b</sup> Collaborative Innovation Center of Chemical Science and Engineering (Tianjin), Tianjin 300072,  
China

<sup>c</sup> Joint School of National University of Singapore and Tianjin University, International Campus of  
Tianjin University, Binhai New City, Fuzhou, 350207, P. R. China

<sup>d</sup> Chemistry and Chemical Engineering Guangdong Laboratory, Shantou, 515031, China

<sup>e</sup> Tianjin Key Laboratory of Membrane Science and Desalination Technology, Tianjin University,  
Tianjin 300072, China

\* E-mail: wuhong@tju.edu.cn Tel: 86-22-23500086 Fax: 86-22-23500086

\* E-mail: fspan@tju.edu.cn Tel: 86-22-23500086 Fax: 86-22-23500086

\* E-mail: zhyjiang@tju.edu.cn Tel: 86-22-23500086 Fax: 86-22-23500086

## **1. Experimental procedures**

### **1.1 Preparation of graphene oxide nanosheets**

Graphene oxide (GO) nanosheets were prepared by a modified Hummer's method as described in our previous work.<sup>1</sup> In brief, H<sub>2</sub>SO<sub>4</sub> (115 mL, 98%) was transported to a round-bottom flask and then cooled below 0 °C in a cryogenic reactor. Then 5g of graphite (10000 mesh) and 2.5 g of NaNO<sub>3</sub> was added to the flask, followed by the addition of KMnO<sub>4</sub> (15 g) during a period of at least 30 minutes. After stirring the mixture for 4 hours under the temperature of 35 ± 5 °C, 230 mL of deionized water was added into the solution and the temperature was maintained below 95 °C. The temperature was then raised to 95 °C and remained for 30 min. Afterwards, ultrapure water (1000 mL), H<sub>2</sub>O<sub>2</sub> (30 mL, 98%), HCl (500 mL, 5 wt%) and ultrapure water (1000 mL) were successively added to the liquid mixture. Finally, a yellow-brown GO aqueous dispersion was obtained by ultrasonication of the above product for 1 h and then centrifuging at 10000 rpm to remove the incompletely exfoliated or large portions.

## 2. Characterization

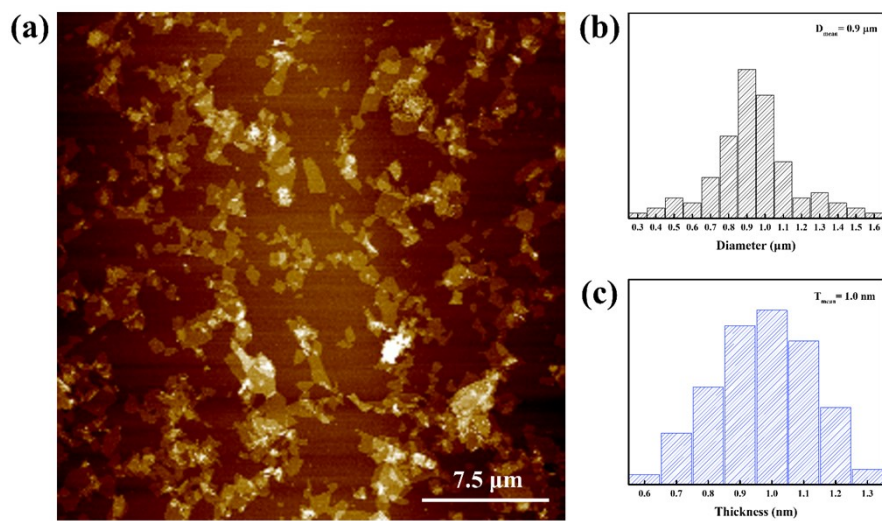


**Fig. S1** (a) AFM image, (b) size distribution and (c) thickness distribution of GO nanosheets.

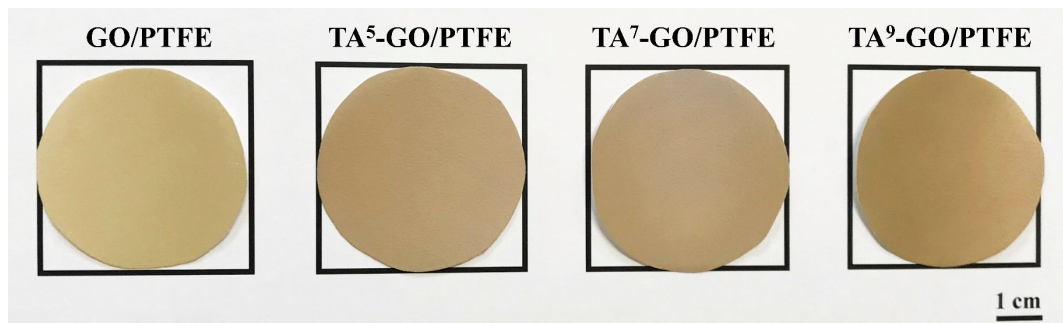


**Fig. S2** Digital photograph of membranes.

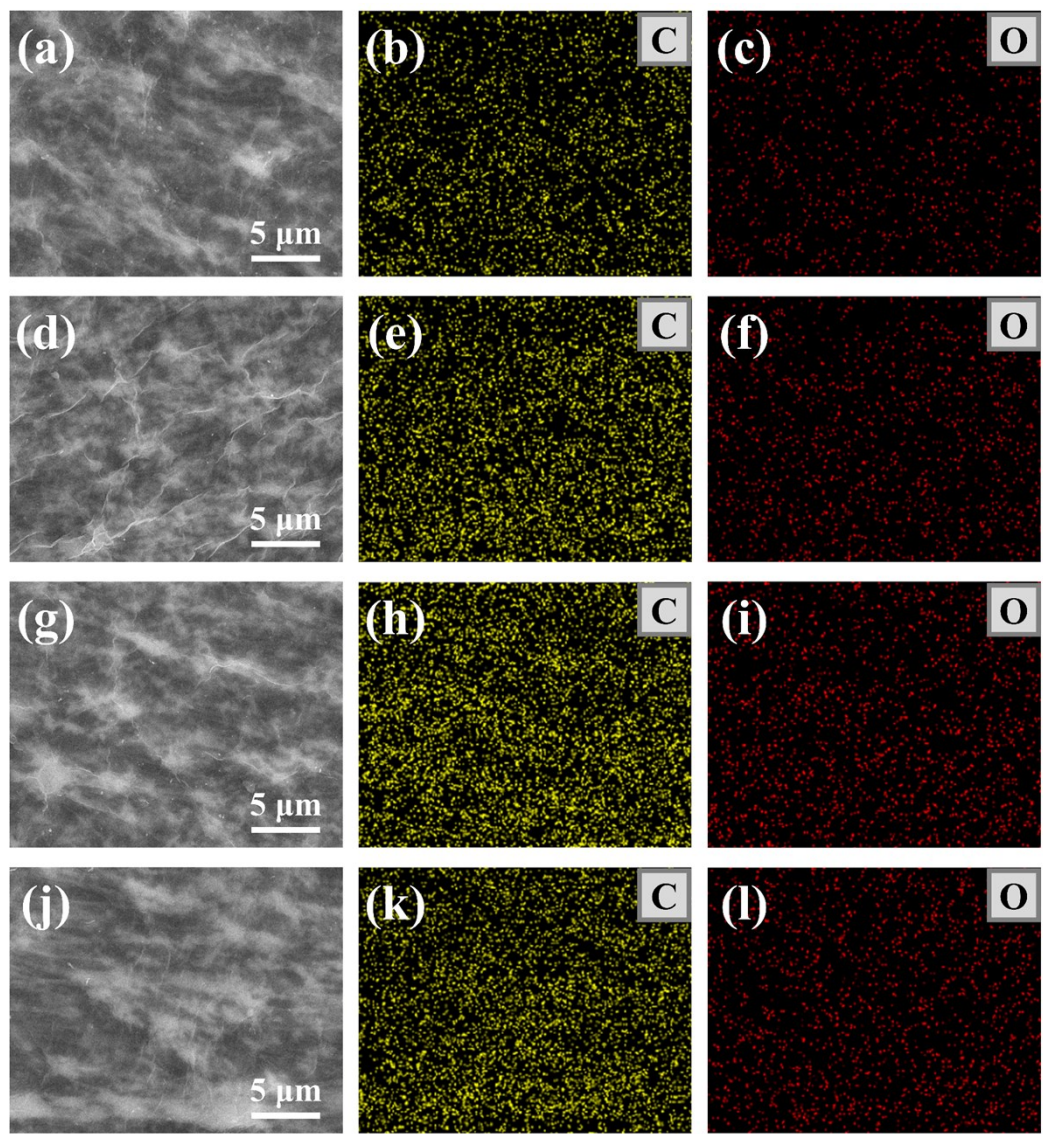


**Fig. S3** SEM surface images and EDS mapping of (a-c) GO/PTFE membrane, (d-f) TA<sup>5</sup>-GO/PTFE membrane, (g-i) TA<sup>7</sup>-GO/PTFE membrane and (j-l) TA<sup>9</sup>-GO/PTFE membrane.

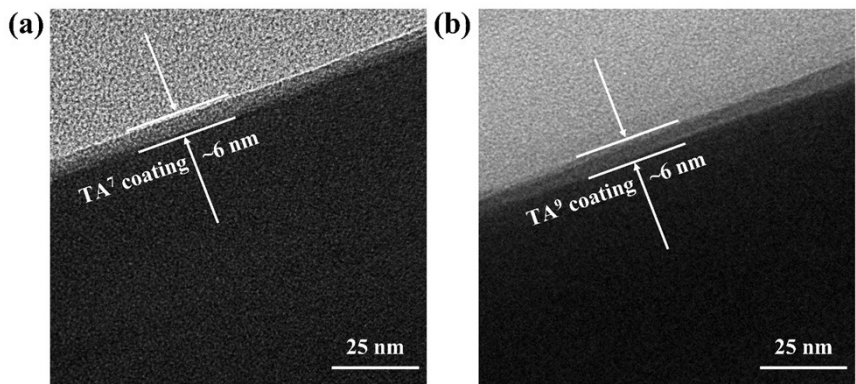


**Fig. S4** Cross-sectional high-resolution TEM images of coatings of (a) TA<sup>7</sup>-GO/PTFE membrane and (b) TA<sup>9</sup>-GO/PTFE membrane.

The cross-sectional TEM samples of TA-GO/PTFE membranes were fabricated by ultramicrotomy. First, The TA-GO/PTFE membranes were cut into rectangles with the average width of 2 mm and then embedded with epoxy resin EPON 812. During ultramicrotomy, an ultramicrotome (Leica EM UC6) fitted with a diamond knife was used to trim down the cutting face of the embedded membrane samples. The membrane samples were cut into thin slices with average thickness of about 80 nm and then picked up with the support films, including the lacey support films and the ultrathin pure carbon film with no formvar backing on lacey carbon support film, from the water trough. Then the as-prepared samples were dried for TEM tests.

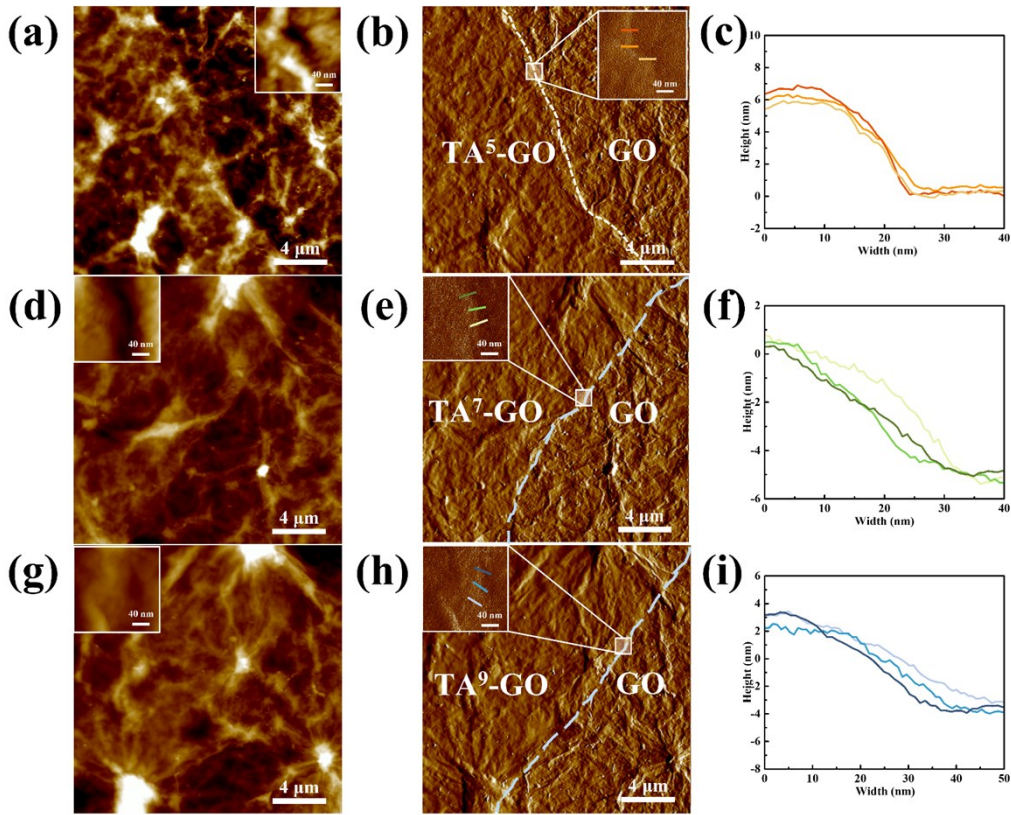


**Fig. S5** AFM images and corresponding height profiles of (a-c)  $\text{TA}^5\text{-GO}/\text{PTFE}$  membrane, (d-f)  $\text{TA}^7\text{-GO}/\text{PTFE}$  membrane and (g-i)  $\text{TA}^9\text{-GO}/\text{PTFE}$  membrane. The left part of each AFM images was covered with TA coatings. The insert images show the amplifying morphology near the boundaries between TA-GO surfaces and bare GO surfaces. The height profiles correspond to the lines in AFM images from left to right.

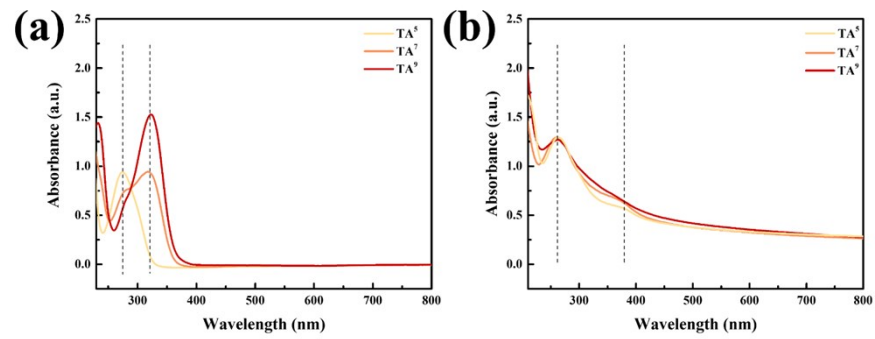


**Fig. S6** UV-vis spectra of TA<sup>5</sup>, TA<sup>7</sup> and TA<sup>9</sup> aqueous solutions (a) before and (b) after the thermal treatment.

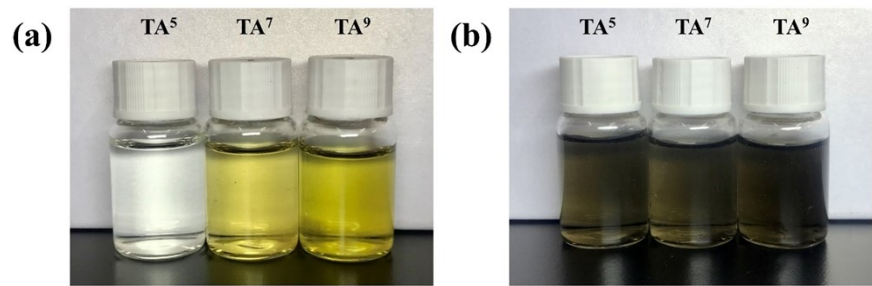


**Fig. S7** Digital pictures of TA<sup>5</sup>, TA<sup>7</sup> and TA<sup>9</sup> aqueous solutions (a) before and (b) after the thermal treatment.

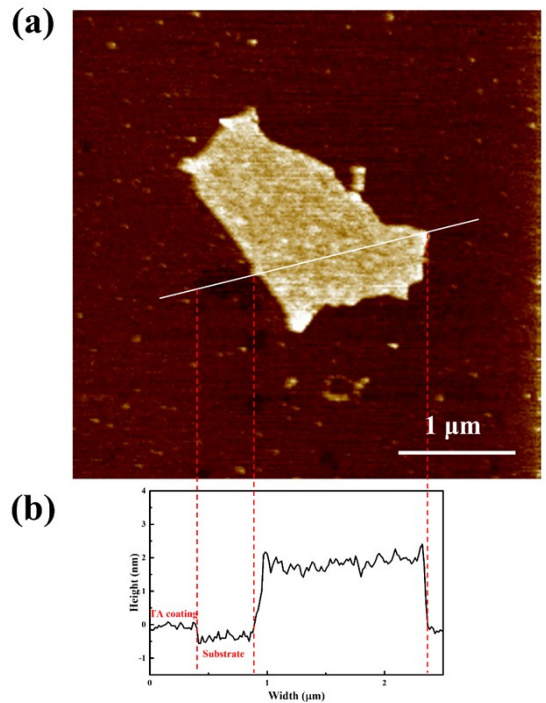


**Fig. S8** (a) AFM image and (b) corresponding height profile of the TA coating and the GO nanosheet.

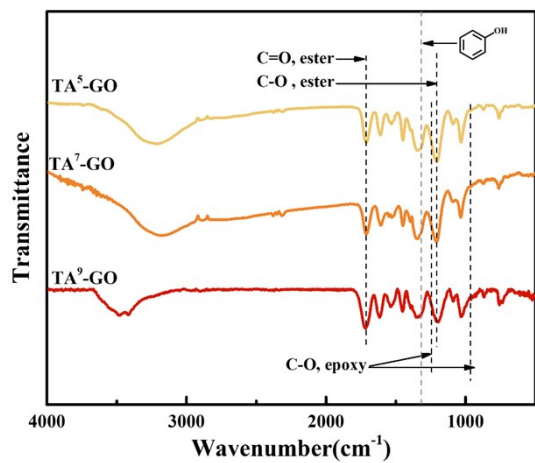


**Fig. S9** FTIR spectra of TA<sup>5</sup>-GO membrane, TA<sup>7</sup>-GO membrane and TA<sup>9</sup>-GO membrane.

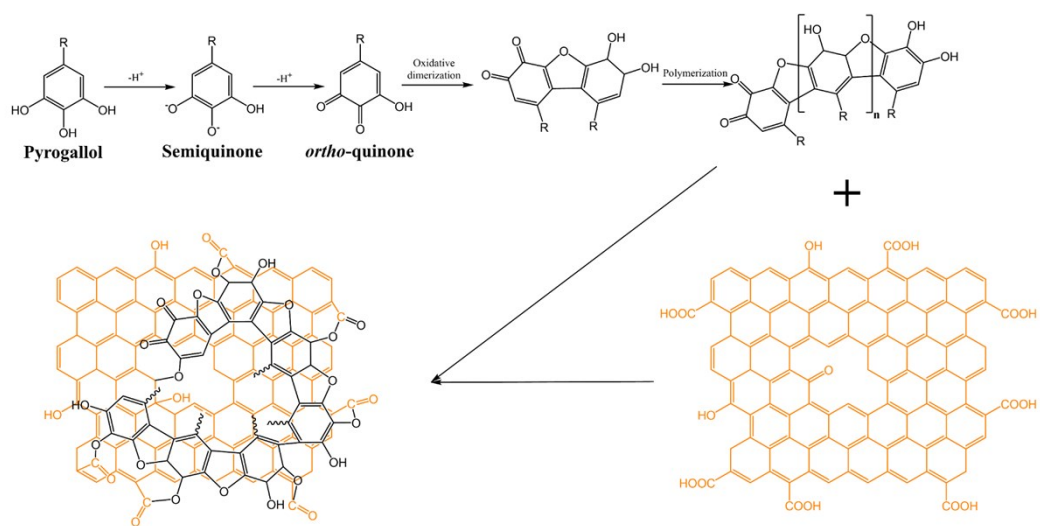


**Fig. S10** Formation mechanism of TA coatings and interfacial sieving layers.

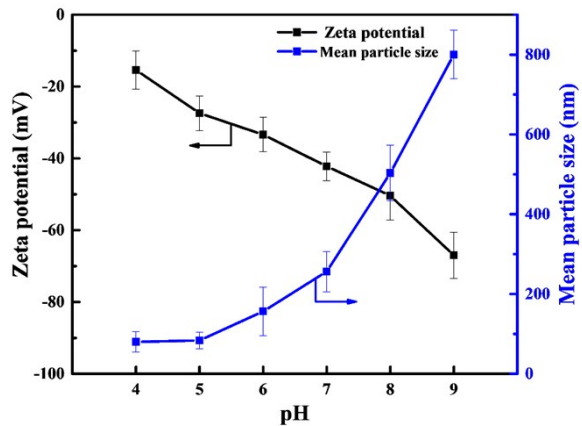


**Fig. S11** (a) Mean particle size and zeta potential of TA aqueous solutions ( $0.2 \text{ mg mL}^{-1}$ ) with different pH values.

**Table S1** The degree of dissociation of phenolic hydroxyl groups under different pH values

pH value	The degree of dissociation of phenolic hydroxyl groups (%)
4.0	~0
5.0	0.03
6.0	0.32
7.0	3.07
8.0	24.03
9.0	75.97

The degree of dissociation of phenolic hydroxyl groups under different pH values was calculated by eqn (1)<sup>2</sup>:

$$pH = pK_a + \log_{10}([A^-]/[HA]) \quad (1)$$

where pH is the pH value of TA solutions;  $pK_a$  is acidity coefficient of TA, 8.5;  $[A^-]$  is the concentration of semi-quinone groups;  $[HA]$  is the concentration of TA.

The proper degree of dissociation of phenolic hydroxyl groups in the TA aqueous solutions is of great importance for the controllable fabrication of the TA coatings. Specifically, the degree of dissociation of phenolic hydroxyl groups in the TA aqueous solutions with the pH value below 5 is less than 0.03%, so the amount of electrophilic and nucleophilic entities is too low for the controllable fabrication of the TA coatings. Furthermore, as the pH value of the TA aqueous solutions is above 9, the degree of dissociation of phenolic hydroxyl groups is higher than 75.97%, resulting in unstable TA solutions with large aggregates. Thus, the pH value of 5, 7, 9 are chosen as representative conditions for exploring the manipulation of the coating structure.

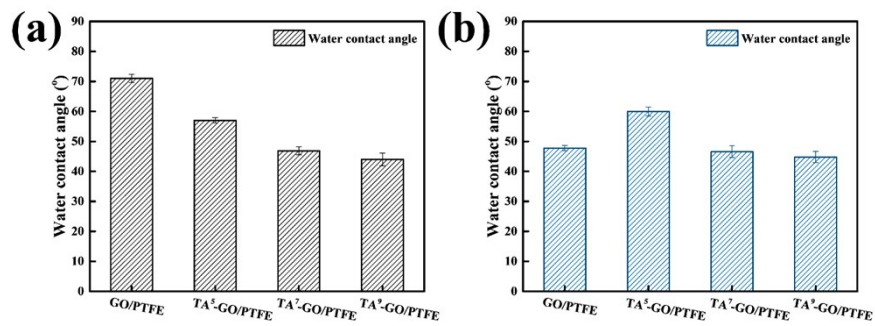


**Fig. S12** Water contact angles of membranes placed (a) in air and (b) in feed solution (90 wt% *n*-butanol and 10 wt% water) for 14 months.

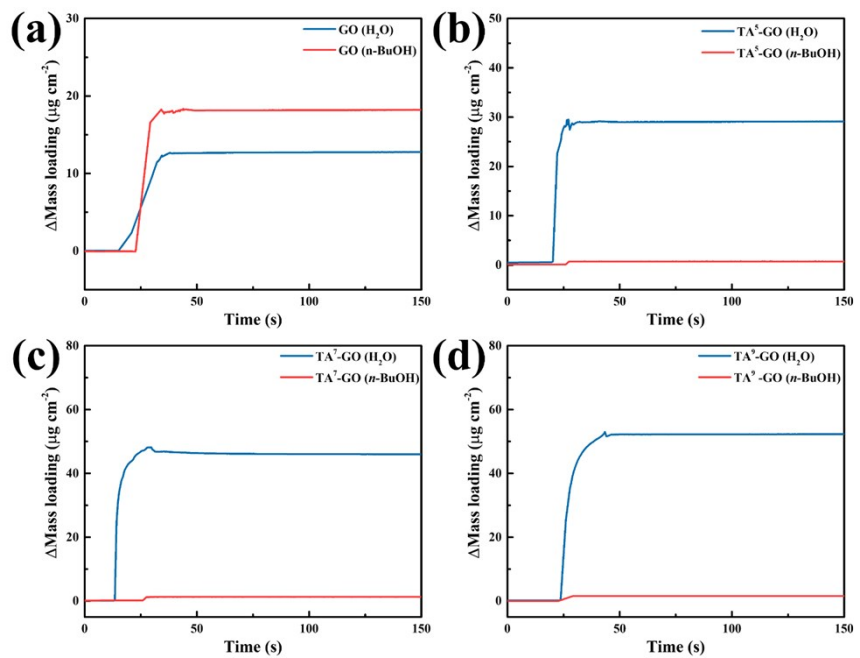


**Fig. S13** Molecule-capture curves of the (a) GO coating, (b)  $\text{TA}^5\text{-GO}$  coating, (c)  $\text{TA}^7\text{-GO}$  coating and (d)  $\text{TA}^9\text{-GO}$  coating.

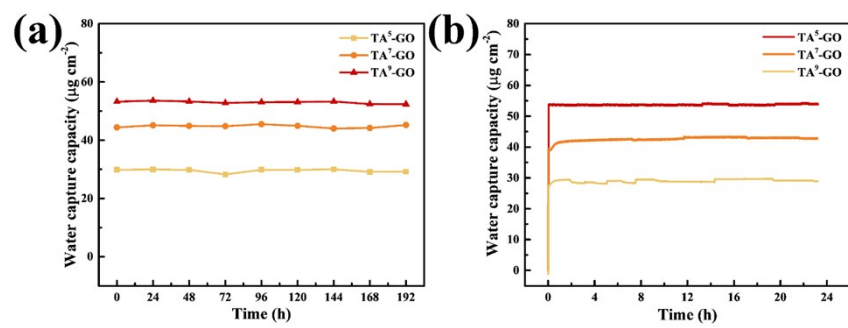


**Fig. S14** Long-term stability of water-capture ability for GO, TA<sup>5</sup>-GO, TA<sup>7</sup>-GO and TA<sup>9</sup>-GO coatings during (a) the batch operation and (b) the continuous operation.

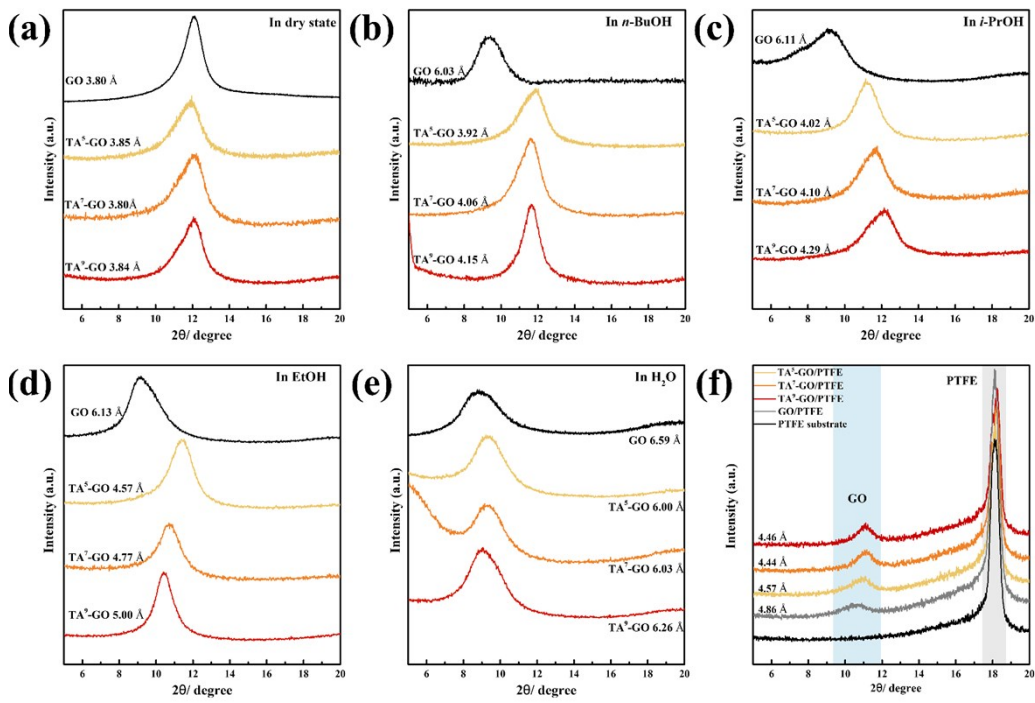


**Fig. S15** XRD patterns of GO, TA<sup>5</sup>-GO, TA<sup>7</sup>-GO, and TA<sup>9</sup>-GO freestanding membranes in (a) dry state and treated by (b) *n*-BuOH; (c) *i*-PrOH; (d) EtOH and (e) H<sub>2</sub>O. (f) GIXRD patterns of GO, TA<sup>5</sup>-GO/PTFE, TA<sup>7</sup>-GO/PTFE, and TA<sup>9</sup>-GO/PTFE composite membranes after the long-term operation.

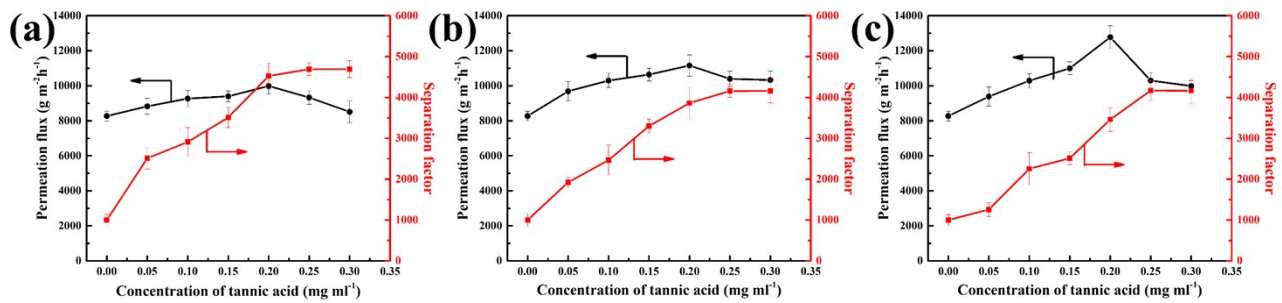


**Fig. S16** Water/*n*-butanol pervaporation separation performance (80 °C) of (a) TA<sup>5</sup>-GO/PTFE, (b) TA<sup>7</sup>-GO/PTFE and (c) TA<sup>9</sup>-GO/PTFE membranes that were fabricated under different TA concentration concentrations.

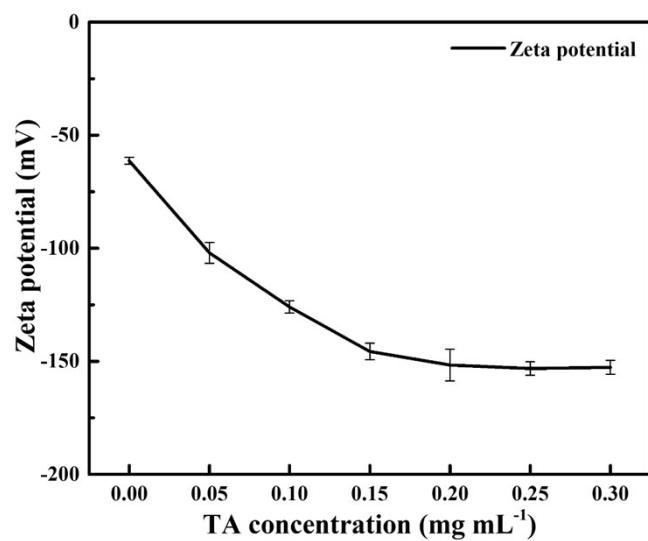


**Fig. S17** Zeta potential of the  $\text{TA}^7\text{-GO/PTFE}$  membranes that were fabricated under different TA concentration.

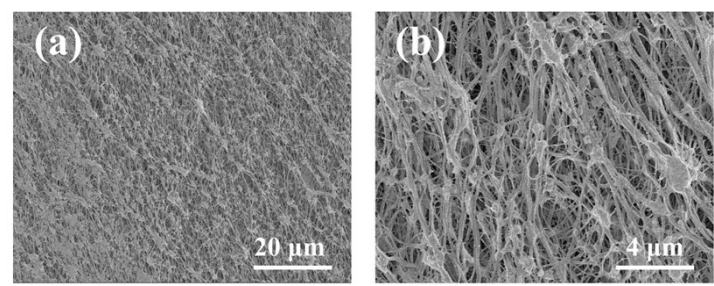


**Fig. S18** SEM image of hydrophilic modified PTFE microfiltration membranes.

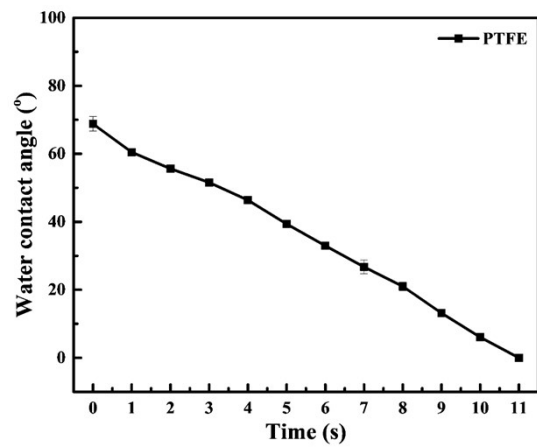


**Fig. S19** Dynamic water contact angle of PTFE microfiltration membranes.

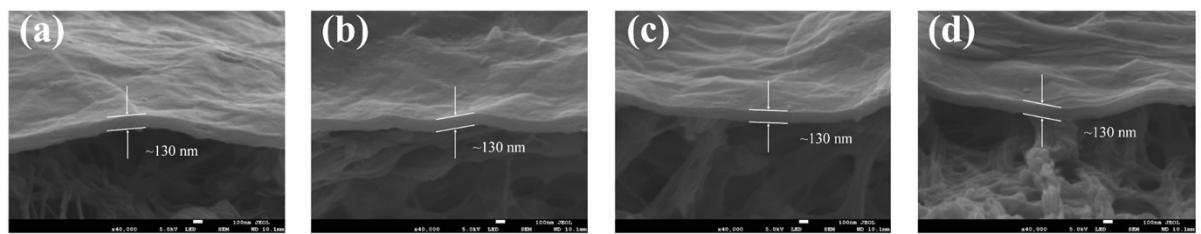


**Fig. S20** Cross-sectional SEM image of (a) GO/PTFE, (b) TA<sup>5</sup>-GO/PTFE, (c) TA<sup>7</sup>-GO/PTFE and (d) TA<sup>9</sup>-GO/PTFE membranes.

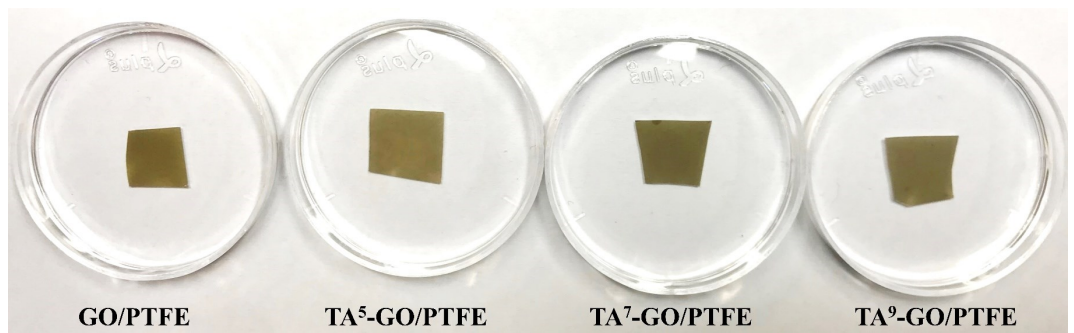


**Fig. S21** Digital photograph of membranes placed in the 90 wt% *n*-butanol aqueous solutions for 14 months.

**Table S2** Comparison of the butanol dehydration performance of TA<sup>5</sup>-GO/PTFE, TA<sup>7</sup>-GO/PTFE and TA<sup>9</sup>-GO/PTFE membranes in this study with literature results.

Membrane material	Feed temperature (°C)	Water concentration in feed (wt %)	Flux g m <sup>-2</sup> h <sup>-1</sup>	Separation factor	Reference
GO membrane	70	10	4340	1791	<sup>4</sup>
GO membrane	70	10	1630	5120	<sup>5</sup>
GO membrane	70	10	10120	1523	<sup>3</sup>
GO membrane	50	10	700	15000	<sup>6</sup>
GO membrane	80	10	9108	2941	<sup>7</sup>
GO membrane	70	20	3510	4454	<sup>8</sup>
Silica membrane	60	6	1500	1000	<sup>9</sup>
Silica membrane	70	5	2300	680	<sup>10</sup>
Silica membrane	60	5	1210	2811	<sup>11</sup>
COF membrane	80	10	8530	3876	<sup>12</sup>
COF membrane	80	10	10573	5534	<sup>13</sup>
COF membrane	80	10	14350	4464	<sup>14</sup>
Zeolite membrane	75	5	2000	1500	<sup>15</sup>
Zeolite membrane	75	5	3430	1300	<sup>11</sup>
MOF membrane	70	5	5380	4280	<sup>16</sup>
MOF membrane	70	15	80	3417	<sup>17</sup>
Polymeric membrane	60	10	2240	1116	<sup>18</sup>
Polymeric membrane	60	15	390	2518	<sup>19</sup>
Polymeric membrane	70	10	1120	1000	<sup>20</sup>
Polymeric membrane	60	15	850	1174	<sup>21</sup>
Polymeric membrane	30	13	2300	3237	<sup>22</sup>
Polymeric membrane	60	15	290	14214	<sup>23</sup>
Polymeric membrane	80	10	2540	2735	<sup>24</sup>
Polymeric membrane	80	10	3610	2764	<sup>25</sup>
TA <sup>5</sup> -GO/PTFE	80	10	9988	4424	This Work
TA <sup>7</sup> -GO/PTFE	80	10	11156	3862	This Work
TA <sup>9</sup> -GO/PTFE	80	10	12771	3460	This Work

1. G. W. He, M. Z. Xu, J. Zhao, S. T. Jiang, S. F. Wang, Z. Li, X. Y. He, T. Huang, M. Y. Cao, H. Wu, M. D. Guiver and Z. Y. Jiang, *Adv Mater*, 2017, **29**, 1605898.
2. I. Erel-Unal and S. A. Sukhishvili, *Macromolecules*, 2008, **41**, 3962-3970.
3. K. Huang, G. P. Liu, J. Shen, Z. Y. Chu, H. L. Zhou, X. H. Gu, W. Q. Jin and N. P. Xu, *Adv Funct Mater*, 2015, **25**, 5809-5815.
4. C. H. Tsou, Q. F. An, S. C. Lo, M. De Guzman, W. S. Hung, C. C. Hu, K. R. Lee and J. Y. Lai, *J Membrane Sci*, 2015, **477**, 93-100.
5. G. H. Li, L. Shi, G. F. Zeng, Y. F. Zhang and Y. H. Sun, *Rsc Adv*, 2014, **4**, 52012-52015.
6. J. J. Yang, D. A. Gong, G. H. Li, G. F. Zeng, Q. Y. Wang, Y. L. Zhang, G. J. Liu, P. Wu, E. Vovk, Z. Peng, X. H. Zhou, Y. Yang, Z. Liu and Y. H. Sun, *Adv Mater*, 2018, **30**, 1705775.
7. Y. M. Song, R. Li, F. S. Pan, Z. He, H. Yang, Y. Li, L. X. Yang, M. D. Wang, H. J. Wang and Z. Y. Jiang, *J Mater Chem A*, 2019, **7**, 18642-18652.
8. Y. Y. Mao, Q. B. Huang, B. C. Meng, K. Zhou, G. P. Liu, A. Gugliuzza, E. Drioli and W. Q. Jin, *J Membrane Sci*, 2020, **611**, 118364.
9. B. Bettens, A. Verhoef, H. M. van Veen, C. Vandecasteele, J. Degreve and B. Van der Bruggen, *Comput Chem Eng*, 2010, **34**, 1775-1788.
10. A. W. Verkerk, P. van Male, M. A. G. Vorstman and J. T. F. Keurentjes, *Sep Purif Technol*, 2001, **22-3**, 689-695.
11. B. X. Huang, Q. Liu, J. Caro and A. S. Huang, *J Membrane Sci*, 2014, **455**, 200-206.
12. H. Yang, L. X. Yang, H. J. Wang, Z. Xu, Y. M. Zhao, Y. Luo, N. Nasir, Y. M. Song, H. Wu, F. S. Pan and Z. Y. Jiang, *Nat Commun*, 2019, **10**, 1-10.
13. H. J. Wang, L. Chen, H. Yang, M. D. Wang, L. X. Yang, H. Y. Du, C. L. Cao, Y. X. Ren, Y. Z. Wu, F. S. Pan and Z. Y. Jiang, *J Mater Chem A*, 2019, **7**, 20317-20324.
14. H. Yang, H. Wu, Y. M. Zhao, M. D. Wang, Y. M. Song, X. X. Cheng, H. J. Wang, X. Z. Cao, F. S. Pan and Z. Y. Jiang, *J Mater Chem A*, 2020, **8**, 19328-19336.
15. F. Zhang, L. N. Xu, N. Hu, N. Bu, R. F. Zhou and X. S. Chen, *Sep Purif Technol*, 2014, **129**, 9-17.
16. X. L. Liu, C. H. Wang, B. Wang and K. Li, *Adv Funct Mater*, 2017, **27**, 1604311.
17. G. M. Shi, T. X. Yang and T. S. Chung, *J Membrane Sci*, 2012, **415**, 577-586.
18. T. Liu, Q. F. An, Q. Zhao, K. R. Lee, B. K. Zhu, J. W. Qian and C. J. Gao, *J Membrane Sci*, 2013, **429**, 181-189.
19. N. Widjojo and T. S. Chung, *Chem Eng J*, 2009, **155**, 736-743.
20. Y. X. Zhu, S. S. Xia, G. P. Liu and W. Q. Jin, *J Membrane Sci*, 2010, **349**, 341-348.
21. Y. Wang, S. H. Goh, T. S. Chung and P. Na, *J Membrane Sci*, 2009, **326**, 222-233.
22. S. Kalyani, B. Smitha, S. Sridhar and A. Krishnaiah, *Carbohydr Polym*, 2006, **64**, 425-432.
23. Y. M. Xu and T. S. Chung, *J Membrane Sci*, 2017, **531**, 16-26.

24. H. Yang, H. Wu, Z. Xu, B. W. Mu, Z. X. Lin, X. X. Cheng, G. H. Liu, F. S. Pan, X. Z. Cao and Z. Y. Jiang, *J Membrane Sci*, 2018, **561**, 79-88.
25. G. H. Liu, Z. Y. Jiang, H. Yang, C. D. Li, H. J. Wang, M. D. Wang, Y. M. Song, H. Wu and F. S. Pan, *J Membrane Sci*, 2019, **572**, 557-566.